Atomic-scale model of *c*-Si/*a*-Si:H interfaces

M. Tosolini,[1,2] L. Colombo,[2,3] and M. Peressi[1,2,*]
[1]*Dipartimento di Fisica Teorica, Università di Trieste, Strada Costiera 11, I-34014 Trieste, Italy*
[2]*INFM DEMOCRITOS National Simulation Center, Trieste, Italy*
[3]*Dipartimento di Fisica, Università di Cagliari, Cittadella Universitaria, I-09042 Monserrato (CA), Italy*
(Received 21 January 2003; revised manuscript received 7 July 2003; published 4 February 2004)

We present the first atomic-scale numerical study of the *c*-Si/*a*-Si:H interface structure, based on combined tight-binding molecular dynamics simulations and *ab initio* electronic structure calculations. We generate models with different realistic H concentrations, up to 11%, following two distinct procedures. We discuss the effects on the topological and electronic properties due to the H content and to the different generation protocols. We obtain model junctions with a realistic percentage of topological defects and showing either a trend to amorphization of the *c*-Si region or a trend to recrystallization of the *a*-Si:H region. These are indications of the variety and complexity of the processes present in the real samples, and also suggest that our numerical samples are representative of some realistic cases.

DOI: 10.1103/PhysRevB.69.075301 PACS number(s): 61.43.Dq, 68.35.−p

I. INTRODUCTION

Si-based heterostructures are of enormous technological importance for their use in solar cells and in other optoelectronic devices. Compared to high-quality *c*-Si, the use of hydrogenated amorphous silicon (*a*-Si:H) as active element in the solar cells has several advantages from the technological point of view: larger absorption coefficient in the solar spectrum which requires a smaller thickness (≈ 1 versus $\approx 20\ \mu$m), possibility of deposition on larger surfaces (up to $\approx 1\ \mathrm{m}^2$), and lower cost of fabrication. With respect to pure *a*-Si, the hydrogenated material is preferable for its lower content of coordination defects, which could prevent doping and photoconductivity.[1]

In the present work we focus our attention on interfaces between *a*-Si:H and the pure crystalline phase *c*-Si/*a*-Si:H. The electronic properties of this interface have been investigated experimentally with a variety of techniques, giving some conflicting results. For instance, the reported values of the band lineups, which are key parameters governing the electronic and optical properties, range from 0 to 0.7 eV for typical H content of about 10–15 % (see Ref. 2, and references therein).

In absence of a direct experimental knowledge of the atomic-scale structure, a theoretical/computational study of the interface is appropriate. Despite the wide literature concerning the simulation and the study of the amorphous phase, both pure and hydrogenated, either from first principles[3] and by means of semiempirical approaches,[4–7] we are not aware of any direct simulation of the *c*-Si/*a*-Si:H interface. Instead, we are aware of a couple of computational investigations concerning the band alignment at this interface[8,9] obtained by means of a comparison of the two phases separately. On the other side, direct simulations of the interface concerning only the nonhydrogenated case, namely, *c*-Si/*a*-Si, have been published in Refs. 10–13. The presence of hydrogen corresponds to a more realistic situation, and therefore the study of *c*-Si/*a*-Si:H interface is worthy.

A direct atomic-scale simulation of the interface is aimed at clarifying first of all several questions concerning its structural and electronic properties. In the present paper we focus on the generation of trustworthy interface model and on the investigation of the related topological properties, including the interface structure and extension, as well as the preferential distribution of hydrogen. We study some selected configurations, with interfaces obtained following two different simulation protocols, and with different hydrogen concentrations, ranging from 3.75 to 11.25 %. A realistic model of the interface is also necessary to afford the study of the electronic properties, including band discontinuities and their dependence on the actual interface structure, on the average hydrogen concentration and on its distribution. We present here only a partial study of the electronic properties. A more detailed investigation will be the subject of a future work.

In the next section we give some technical details concerning the generation of the atomistic structure, which is based on a tight-binding molecular dynamics (TBMD) approach[14] with the use of periodically repeated supercells. We will also describe the two different simulation protocols used to build the interface.

Section III is devoted to the accurate discussion of the results for the *c*-Si/*a*-Si:H interface with 11% of H atomic concentration. In Sec. IV we mention the *ab initio* approach followed for the electronic structure calculations, and we briefly presents some results for the density of states (DOS) of that sample. Finally in the last section we summarize and compare the results obtained for other samples with different H concentrations.

II. GENERATION OF THE NUMERICAL MODELS

The interatomic interactions are described using a semiempirical, orthogonal, and two-center tight-binding approach, with a minimal basis set containing Si sp^3 and H $1s$ atomic orbitals. The TB matrix elements are parametrized and scaled analytically with the interatomic distance. We list the main references for the different parametrization used here and we refer the reader to the cited articles for details. The parametrization for Si-Si interaction is the one proposed by Goodwin, Skinner, and Pettifor (GSP),[15] and already suc-

 ©2004 The American Physical Society

cessfully applied in different studies concerning amorphous phases.[5,16] The parametrization of Si-H interactions is taken from Ref. 17, a choice motivated by the good results obtained in the application to the problem of H bonding and migration in a-Si,[5] which are in excellent agreement with accurate *ab initio* results. The H-H interaction has been described as in Ref. 18. The cutoffs are 2.8, 2.5, and 3.1 Å, respectively, for Si-Si, Si-H, and H-H interactions.

Heterostructures can be conveniently described using periodically repeated supercells, as proposed, for instance, in Ref. 19, containing one slab of each constituent and therefore two interfaces. In the present case we want to simulate the most common case, i.e., interfaces obtained with deposition of a-Si:H on a (001) Si substrate. Therefore we consider tetragonal (001) supercells containing up to 320 Si atoms, with $a=b=2a_0$ and $c\approx 10a_0$, where a_0 is the lattice parameter of the crystalline phase. The lateral dimensions a and b are fixed to simulate the growth on a c-Si substrate, and the c/a ratio is optimized for each system (at a given H concentration) according to the equilibrium density of the amorphous slab.

Once the optimal c/a is determined, the dynamical evolution of the system is within the constant volume, constant temperature ensemble. Atomic trajectories have been aged by means of the velocity-Verlet algorithm, using a time step as short as 0.5 fs. Temperature control has been operated by velocity rescaling.

Some considerations concerning density and internal stress are now in order. Experimentally the density of c-Si at 0 K is $\rho_c=2.33$ g cm^{-3}, equivalent to a lattice parameter $a_0=5.429$ Å.[8] The GSP parametrization gives an equilibrium density $\rho_c^{\mathrm{GSP}}=2.35$ g cm^{-3}, corresponding to a lattice parameter $a_0^{\mathrm{GSP}}=5.41$ Å, $\approx 0.3\%$ less than the experimental value. Conversely, if the lattice parameter is fixed to the experimental value, an internal stress of about -250 MPa is obtained with GSP parametrization for the system at room temperature. Experimentally a-Si:H is less dense than a-Si,[20] by an amount which depends on the H concentration. We tested that the variation of the calculated equilibrium density of a-Si:H with the H content is similar to the experimental one. Therefore in our numerical models we use the experimental values for the density, i.e., 2.20, 2.24, 2.28 g cm^{-3} for atomic H concentration equal to 11.25, 7.5, and 3.75 %, respectively (2.32 g cm^{-3} extrapolating to pure a-Si). The numerical samples of a-Si:H obtained with these values of the density and with the parametrizations chosen here have a residual internal stress of the order of magnitude of 10^2 MPa,[21] similar to the one obtained for pure a-Si and c-Si.

Hydrogenated Si samples have been obtained by quenching from melt as sketched in Figs. 1 and 2. The quenching from melt protocol and the creation of the a-Si:H starting point structure corresponds to the first ≈ 30 ps in both Figs. 1 and 2. In practice, we start from a crystalline Si and we heat it up to 6000 K in ≈ 1 ps (heating rate: $\sim 6\times 10^{15}$ K/s) in order to obtain a very disordered configuration in a reasonable time. After a short thermalization the system is rapidly cooled down close to the melting temperature (≈ 1800 K). A number of H atoms corresponding to the desired concentration is now added randomly to this melt, under the only condition that the interatomic Si-H distances are greater then 1 Å. At this stage, after the hydrogenation, we can proceed following two different procedures, represented in Figs. 1 and 2, respectively.

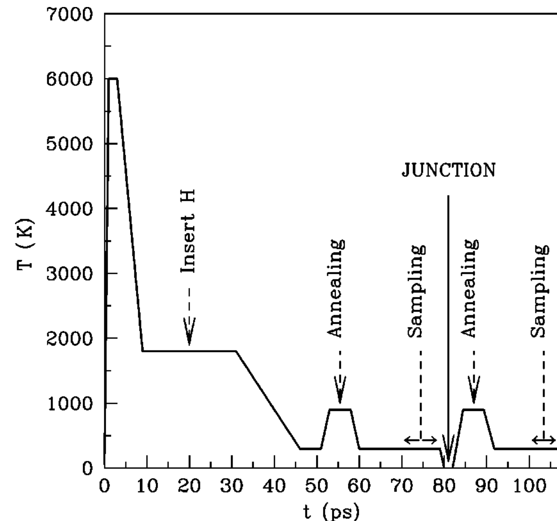

FIG. 1. Protocol followed for the generation of the c-Si/a-Si:H interface through a tight-binding molecular dynamics approach, according to the method A described in the text.

The first method (A, Fig. 1) is a sort of cut and paste. (i) We separately generate a sample of a-Si:H as explained, in a tetragonal cell with dimensions $a=2a_0$, $c\approx 5a_0$ (the actual value depending on the H content as discussed above). (ii) The system is cooled at room temperature (RT), then annealed at ≈ 900 K for few ps; the system is further equilibrated at RT for 10 ps and then the statistical averages are taken for 5–10 ps to check the quality of the sample. (iii) We join this cell through the smallest face with one of the same size of pure c-Si, at low temperature; this junction must be done carefully, avoiding that some boundary atoms come too close together. (iv) The internal degrees of freedom of the structure are then relaxed first at low temperature, with a reduced time step (0.1 fs), and then through a careful thermal

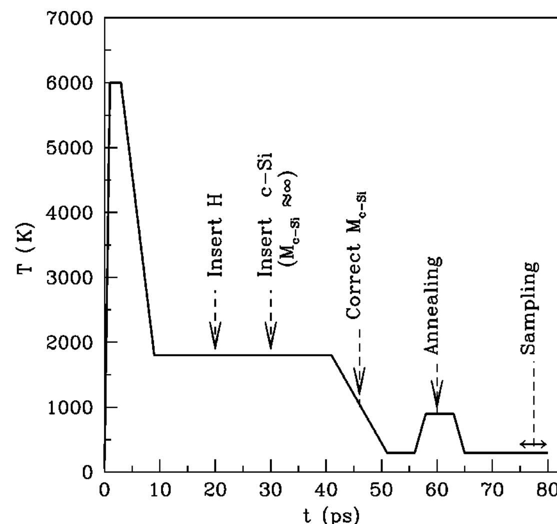

FIG. 2. As in Fig. 1, but for method B.

TABLE I. Dimensions of the tetragonal cells used for *c*-Si and *a*-Si:H slabs with different atomic H concentration (before the junction) in method A. N_{Si} and N_H are the number of Si and H atoms, and the atomic H concentration reported in the first column is the ratio N_H/N_{Si}. The dimensions in the directions parallel to the substrate are $a=b=10.859$ Å for any simulation cell.

Sample (% H)	N_{Si}	N_H	c (Å)	c/a
c-Si	160		27.149	2.50
a-Si:H (3.75%)	160	6	27.692	2.55
a-Si:H (7.5%)	160	12	28.235	2.60
a-Si:H (11.25%)	160	18	28.778	2.65

annealing up to 900 K. Finally, the system is equilibrated for 10 ps at 300 K. In Table I we summarize the size of the tetragonal cells used for *c*-Si and *a*-Si:H in method A before the junction.

The second method (B, Fig. 2) is a more direct generation of the interface, whose formation starts already in the quenching from melt phase of the simulation, before cooling and equilibrating the *a*-Si:H structure. (i) As in method A we generate a disordered *a*-Si:H structure. (ii) While keeping the structure at high temperature (1800 K) we add a slab of *c*-Si. We therefore start creating the amorphous-crystalline interface at this stage, proceeding for about 10 ps with the amorphization process of a portion only of a simulation cell. In practice this is obtained with a damped dynamics of the (nominally) *c*-Si atoms, by setting their atomic masses at a fictitious large value. (iii) Then the sample is cooled down to RT, all the masses are reported at their proper values, and a good crystalline/amorphous structure is indeed obtained. (iv) We perform an annealing at 900 K followed by an equilibration at RT.

Instead of setting fictitious large masses for the amorphization of a portion of the structure, another possibility would be to use a strong gradient temperature, but we think this is a worse approximation of the experimental conditions.[13] A quite "standard" protocol for the creation of an interface is to start from the beginning with the entire simulation cell and to do the amorphization of a portion only: the results should not be substantially different from our method B, which is more efficient and cheaper since it allows us to manage with only half of the number of atoms for a considerably long time of the simulation (~30 ps in our units).

The final *a*-Si:H/*c*-Si structures, obtained both from methods A and B, contain 320 Si atoms and a number of H atoms varying up to 18 (see Table I). Our two methods are aimed at obtaining two, possibly different, realistic samples of the structure for any H concentration. In particular, a different distribution of the light, more diffusive, H atoms can be expected, as well as possible variations in the defect concentration and in the extension of the interface regions.

III. STRUCTURAL CHARACTERIZATION OF THE NUMERICAL SAMPLES

In this section we focus directly on the structural analysis of the heterostructures. We only report that we had also performed a careful structural analysis of the *a*-Si:H sample *before* the junction in method A, to check the quality of our computer generated models step by step: the results obtained for the pair correlation function, angular distribution, velocity distribution, etc., are of good quality compared with experimental data[22] and previous calculations.[3,5]

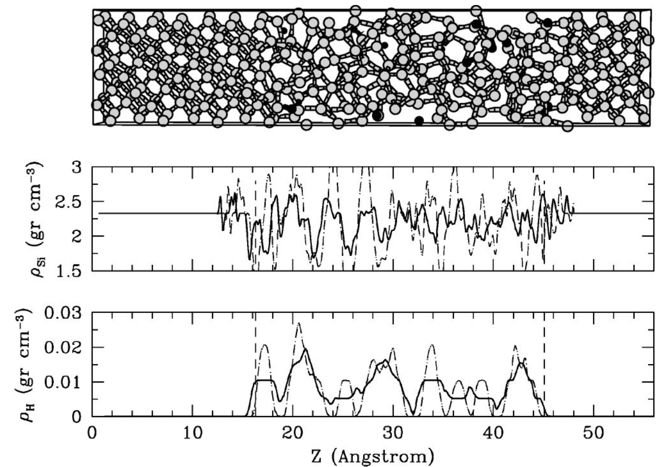

FIG. 3. Upper panel: Snapshot of the heterostructure simulating the *c*-Si/*a*-Si:H interface with 11.25% of atomic H concentration, obtained with method A. The tetragonal cell contains 320 Si (gray) atoms and 18 H (black) atoms. Lower panels: Mass density profiles of Si and of H, respectively, along the growth direction z of the heterostructure. Solid and dotted-dashed lines are obtained filtering the planar profiles with a window of $a_0/2$ and $a_0/4$, respectively. Vertical dashed lines indicate the initial nominal position of the interface.

We show the ball-and-stick representation of the tetragonal cell simulating the structure with 11.25% of atomic H concentration, obtained with method A in the upper panel of Fig. 3. The tetragonal cell contains 320 Si atoms and 18 H atoms. In the lowest part of the figure we report the mass density profiles of Si and of H, respectively, in the heterostructure along the growth direction z. Vertical long-dashed lines indicate the nominal initial position of the interface, i.e., the junction between the two cells of *c*-Si and *a*-Si:H. The profiles are more precisely macroscopic averages,[19] obtained filtering the planar profiles along z with a window of fixed length L or, equivalently, filtering a three-dimensional quantity with a slab of dimensions $a\times b\times L$. In the present case, dotted-dashed and solid lines are obtained with $L=a_0/4$ and $a_0/2$, respectively. Since $a_0/4$ is the natural periodicity of *c*-Si along the (001) direction, we obtain (as expected) that such profiles are flat in the crystalline regions and have the values of the bulk *c*-Si, and they fluctuate in the amorphous region because of the intrinsic lack of periodicity. The amplitude of such fluctuations cannot give quantitative information because of the statistical noise due to the limited size of the averaging slab. However, the density profiles are a first visual indication of the transition between amorphous and crystalline regions.

We point out that with respect to the initial nominal position of the interface, the density profile of Si indicates the *a*-Si:H/*c*-Si phase boundary has propagated towards the crystalline part. The bottom panel shows that H remains confined

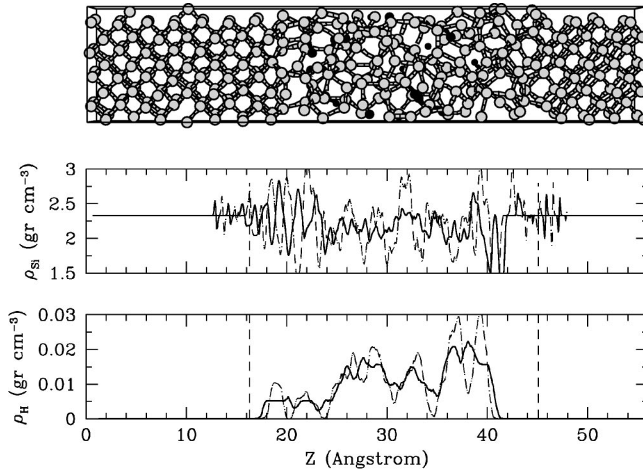

FIG. 4. As in Fig. 3, but for the sample obtained with method B.

within the amorphous region also after the junction and the annealing even if during the simulation we have observed large displacements of H around the interface regions (much larger, in fact, than those predicted by the estimated mobility factor at the corresponding temperature).

Figure 4 is similar to Fig. 3, but for the sample obtained with method B. We can see that in case B the fluctuations of the Si density profiles in the interface regions are less pronounced than in case A, suggesting a partial recrystallization of the amorphous region. Furthermore H is concentrated in a more restricted amorphous region. Both simulations seem to suggest that hydrogen does not have a preferential distribution (e.g., close to the interface, rather than far from it).

In the left panel of Fig. 5 we report the plot of the trajectories of Si and H atoms of the c-Si/a-Si:H heterostructure shown in Fig. 3, during the sampling at 300 K, projected onto a xz plane. On the right side, we report the main structural functions [pair correlation function $g_{\text{Si-Si}}(r)$, angle distribution function $g_{\text{Si-Si-Si}}(\theta)$] of the heterostructure, averaged over slabs of about $a_0/2$. These properties provide a quantitative estimate of the interface extension, about 8 Å. We stress that in the middle regions of the two phases, far from the interface, the structural functions have recovered the bulklike behavior of c-Si and a-Si:H, and this stands for the appropriate size of the supercell. We also studied the pair correlation functions related to the presence of H, namely, $g_{\text{Si-H}}(r)$ and $g_{\text{H-H}}(r)$: they are less meaningful then $g_{\text{Si-Si}}(r)$ because of the reduced statistics due to the very few H atoms, but, however, in the middle of the a-Si:H region also these functions have the profiles typical of the bulk a-Si:H. The comparison with the same figures for the interface obtained with method B (Fig. 6) further indicates the trend of a partial recrystallization of the amorphous region.

In Table II we report the relative occurrence of undercoordinated (with dangling bonds) and overcoordinated (with floating bonds) Si atoms in the amorphous slab and in the two interface regions (average of the two in each supercell), as well as the average coordination number and the amount of Si atoms used for the statistics in those regions. The two interface regions have a similar extension in both samples A and B, ~8 Å in the growth direction, and hence include

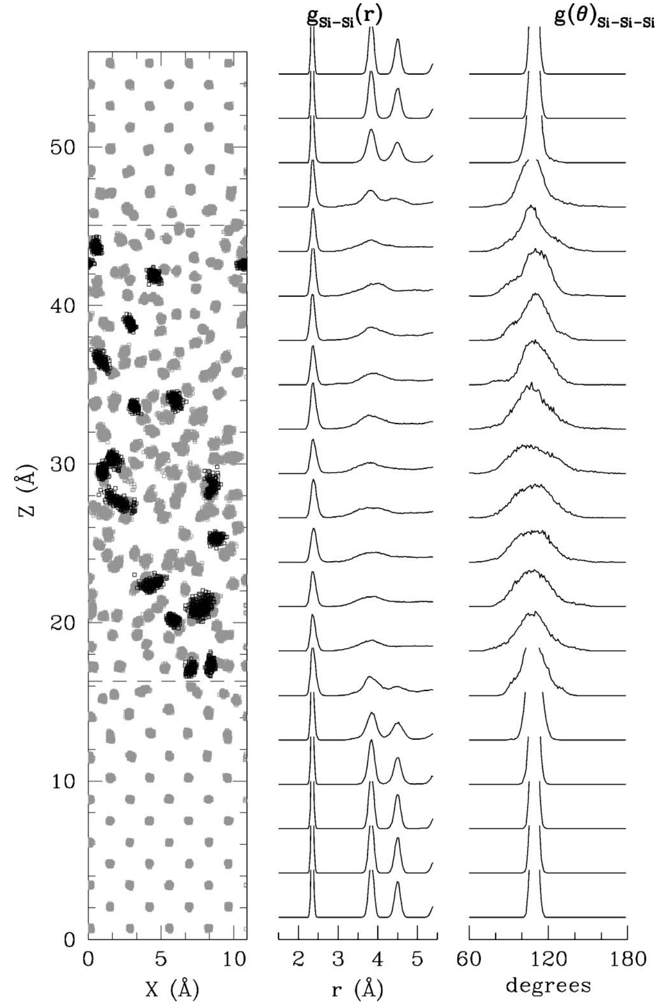

FIG. 5. From left to the right: plot of the trajectories of Si (gray) and H (black) atoms of the c-Si/a-Si:H heterostructure shown in Fig. 3, during the sampling at 300 K, projected onto a xz plane; structural functions (pair correlation function, angle distribution function) averaged over slabs of about $a_0/2$.

~45–50 Si atoms. The amorphous slab is less extended in sample B than in A because of the partial recrystallization occurred. The coordination of Si atoms is calculated simply using a bond-cutoff distance 15% larger than the crystalline bond length for the Si-Si bonds and similarly a bond-cutoff distance 15% larger than the Si-H distance in the silane molecule for the Si-H bonds. This choice is consistent with the actual position of the first minimum of the corresponding pair correlation functions computed in the amorphous slab. For our present purposes a classification of coordination defects based on pure geometrical criteria is sufficient, but we point out that a better characterization of the bonding configuration and a resolution of possible ambiguities of related topological defects[25] can be obtained only by an accurate analysis of the valence charge distribution and more sophisticated methods based on the "electron localization function"[26] or Wannier functions.[27]

In the structures that we are considering here, the percentage of defects is realistic and comparable with the percent-

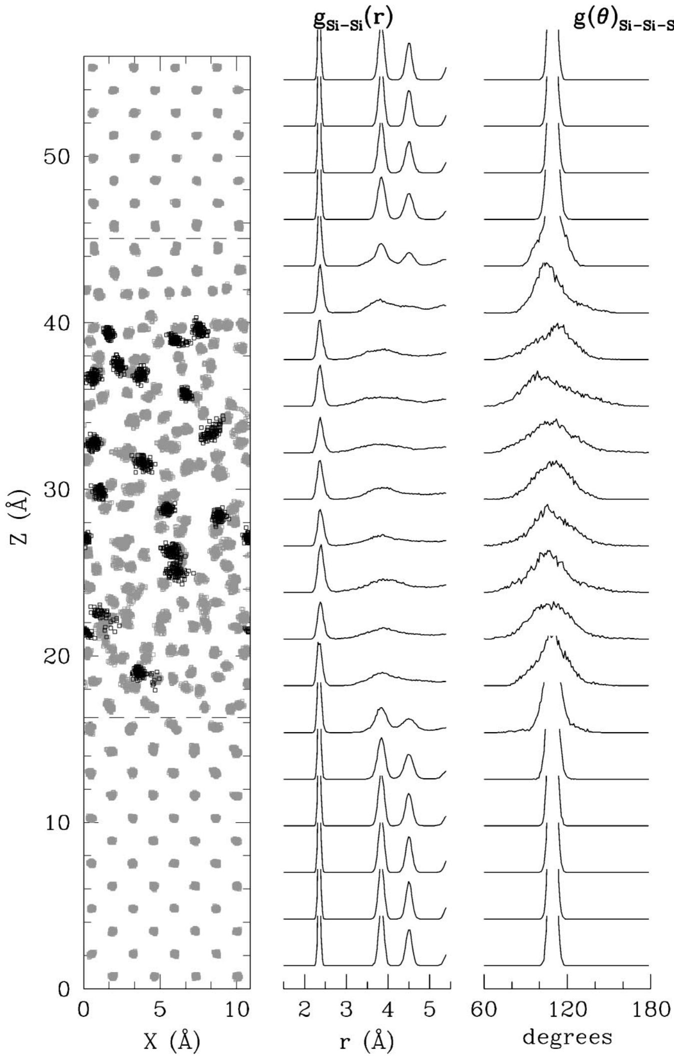

FIG. 6. As in Fig. 5, but for the sample obtained with method B.

ages reported in the literature. In the interface region is typically smaller than in the amorphous part.

Although no dramatic differences in the relative occurrence of defects are observed comparing A and B models, the quality of structures obtained with method B seems generally better, being characterized by a slightly minor amount of defects, both undercoordinated and overcoordinated, in the amorphous slab and in the interface regions.

IV. ELECTRONIC STRUCTURE

The structures obtained with TBMD can be used as the input of *ab initio* electronic structure calculations. A complete detailed study of the electronic properties of *c*-Si/*a*-Si:H interface is beyond the scope of the present work; however, we present here some results for the density of states, in connection with the topological analysis presented before. Calculations are performed within the framework of density-functional theory in the local density approximation, using norm-conserving pseudopotentials,[29] a plane-wave cutoff of 16 Ry for the plane wave basis set, and a Monkhorst-Pack grid[30] with 4 and 20 **k** points for the self-consistent and non-self-consistent calculations, respectively. This approach has been already successfully used to study the electronic structure of other amorphous Si based systems.[3,10,25]

We report in Fig. 7 the DOS of the sample A with 11.25% of H content, together with the projection over the atoms in the crystalline, amorphous, and interface regions as already specified in Table II. The total DOS of the heterostructure is nonvanishing at the Fermi energy: as one can see from the different contributions, this originates from the amorphous and interface regions (dashed lines) and must be attributed to the existence of the structural defects which are in the present case mainly dangling bonds, as shown in Table II. A part from details due to the possible various origin of the midgap states in different samples, the amorphous-projected contribution has the typical form of the bulk *a*-Si (see, e.g., Ref. 25, and references therein); together with the fact that the *c*-Si projected DOS has the typical profile of bulk *c*-Si, this is a further indication of the appropriate size of our supercell for the description of the junction. Better resolution for the DOS (especially around the Fermi energy) could be obtained improving the technical ingredients of the calculations, such as the number of *k* points, at the cost of a larger computational effort.

TABLE II. Topological defects concentration in the different samples in the *a*-Si:H slab and averaged in the two interface regions in each cell. For each region we report in four columns from the left to the right: undercoordinated ($T_{NN<4}$) atoms; overcoordinated ($T_{NN>4}$) atoms; average coordination number ($\langle NN\rangle$); in parentheses the number of Si atoms considered for the statistics (n_{Si}). NN means "nearest neighbors."

a-Si:H/*c*-Si sample	*a*-Si:H region				interface regions			
(method and % H)	$T_{NN<4}$	$T_{NN>4}$	$\langle NN\rangle$	n_{Si}	$T_{NN<4}$	$T_{NN>4}$	$\langle NN\rangle$	n_{Si}
A (3.25%)	10%	1%	3.88	(116)	2%	2%	4.00	(92)
B (3.25%)	10%	0%	3.90	(111)	2%	0%	3.98	(97)
A (7.5%)	11%	2%	3.91	(110)	6%	1%	3.95	(82)
B (7.5%)	6%	1%	3.95	(112)	4%	0%	3.97	(88)
A (11.25%)	6%	2%	3.95	(121)	6%	0%	3.93	(95)
B (11.25%)	5%	0%	3.93	(93)	3%	0%	3.96	(86)

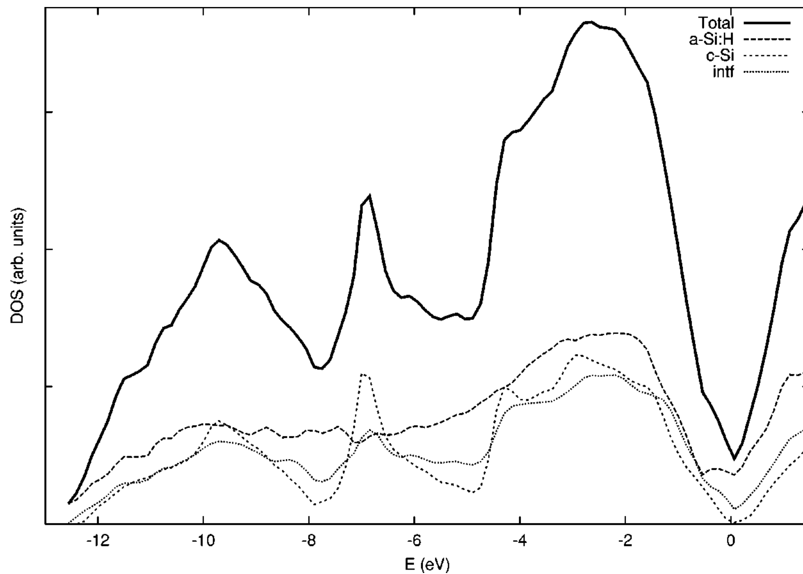

FIG. 7. Electronic density of states of the *a*-Si:H(11%)/*c*-Si sample obtained with method A: total DOS of the heterostructure (thick solid line) and partial DOS projected on amorphous (long-dashed line), interface (short-dashed line), and crystalline (dotted) regions. The normalization of the curves is chosen proportional to the number of atoms considered in the different regions (see Table II for details), and the total DOS coincides with the sum of the three contributions. The Fermi energy is set to zero.

V. CONCLUSIONS

We also study heterostructures with other H concentrations, as summarized in Tables I and II. All our numerical samples contain in general more undercoordinated than overcoordinated defects. It appears from Table II that the percentage of undercoordinated defects is reduced by increasing the amount of H. The effect commonly observed upon hydrogenation of *a*-Si in real samples is a reduction of midgap energy levels, and this is typically ascribed since a long time to the passivation of the dangling bonds by H.[1] In Ref. 25 we demonstrate that a complementary mechanism of reduction of gap states with H is annihilation of overcoordinated defects. The numerical models of interfaces obtained in the present work are consistent with the idea of passivation of the dangling bonds by H, but they do not exclude the possibility of annihilation of floating bonds, which is not evident in the present samples due to their very limited statistics.

A part from the obvious relative differences due to the variations in H content in the different numerical samples, all of the main structural trends previously discussed have been confirmed. In particular we can state the following. (i) A rough estimate of the extension of the interface is $\approx 8-10$ Å, based on the density profiles of Si and H along the growth direction, and on the local pair and angle distribution functions $g_{\text{Si-Si}}(r)$ and $g_{\text{Si-Si-Si}}(\theta)$. (ii) H is almost homogeneously distributed in the amorphous region. (iii) The equilibrium calculated density of the amorphous region is varying with the H content with a trend similar to the experimental data. (iv) Using the two different methods for the generation of the interface, we are able to obtain both a junction with a trend to amorphization of the *c*-Si region (due to the high atomic diffusion during the annealing after the junction in method A) and a junction with a trend to recrystallization[23,24] of the *a*-Si:H region.

In conclusion, we have obtained some atomic-scale models of *c*-Si/*a*-Si:H interfaces for different H contents. The two different trends (amorphization, recrystallization) observed in the interface regions in the samples generated with different procedures, are indications of the variety and complexity of the processes present in the real samples: therefore, it is fair to conclude that our numerical samples are representative of realistic cases and can constitute a reliable input for a further study of the interface electronic properties. Present *c*-Si/*a*-Si:H atomistic models are available for further investigation upon request.

ACKNOWLEDGMENTS

The part of this work concerning the interface electronic structure was done within the ''Iniziativa Trasversale di Calcolo Parallelo'' of the Italian Istituto Nazionale per la Fisica della Materia (INFM) using the parallel version of the PWSCF (Plane-Wave Self-Consistent Field) package (Ref. 28).

*Electronic address: peressi@ts.infn.it

[1] A. Shah, P. Torres, R. Tscharner, N. Wyrsch, and H. Keppner, Science **285**, 692 (1999); B. Rech and H. Wagner, Appl. Phys. A: Mater. Sci. Process. **69**, 155 (1999); E.A. Davis, J. Non-Cryst. Solids **198-200**, 1 (1996); R.A. Street, *Hydrogenated Amorphous Silicon* (Cambridge University Press, Cambridge, 1991).

[2] T.M. Brown, C. Bittencourt, M. Sebastiani, and F. Evangelisti, Phys. Rev. B **55**, 9904 (1997); J.M. Essick, Z. Nobel, Y.M. Li, and M.S. Bennett, *ibid.* **54**, 4885 (1996); A. Fantoni, Y. Vigranenko, M. Fernandes, R. Schwarz, and M. Vieira, Thin Solid Films **383**, 314 (2001); S. Gall, R. Hirschauer, M. Kolter, and D. Bräunig, Sol. Energy Mater. Sol. Cells **49**, 157 (1997); Y.J. Song, M.R. Park, E. Guliants, and W.A. Anderson, *ibid.* **64**, 225 (2000).

[3] F. Buda, G.L. Chiarotti, R. Car, and M. Parrinello, Phys. Rev. B **44**, 5908 (1991); P.A. Fedders and D.A. Drabold, *ibid.* **47**, 13 277 (1993); B. Tuttle and J.B. Adams, *ibid.* **53**, 16 265 (1996); A.A. Valladares, F. Alvarez, Z. Liu, J. Sticht, and J. Harris, Eur. Phys. J. B **22**, 443 (2001).

[4] P. Klein, H.M. Urbassek, and T. Frauenheim, Phys. Rev. B **60**, 5478 (1999).

[5] S. Lanzavecchia and L. Colombo, Europhys. Lett. **36**, 295 (1996).
[6] N. Mousseau and L.J. Lewis, Phys. Rev. B **41**, 3702 (1990); I. Kwon, R. Biswas, and C.M. Soukoulis, *ibid.* **45**, 3332 (1992); J.M. Holender, G.J. Morgan, and R. Jones, *ibid.* **47**, 3991 (1993).
[7] D. Maric and L. Colombo, Europhys. Lett. **29**, 623 (1995).
[8] C. Van de Walle and L.H. Yang, J. Vac. Sci. Technol. B **13**, 1635 (1995).
[9] G. Allan, C. Delerue, and M. Lannoo, Phys. Rev. B **61**, 10 206 (2000); **57**, 6933 (1998).
[10] M. Peressi, L. Colombo, and S. de Gironcoli, Phys. Rev. B **64**, 193303 (2001).
[11] N. Bernstein, M.J. Aziz, and E. Kaxiras, Phys. Rev. B **58**, 4579 (1998); **61**, 6696 (2000).
[12] D.M. Stock, B. Weber, and K. Gärtner, Phys. Rev. B **61**, 8150 (2000).
[13] Cesar R.S. da Silva and A. Fazzio, Phys. Rev. B **64**, 075301 (2001).
[14] L. Colombo, in *Annual Reviews of Computational Physics IV*, edited by D. Stauffer (World Scientific, Singapore, 1996), p. 147, and references therein.
[15] L. Goodwin, A.J. Skinner, and D.G. Pettifor, Europhys. Lett. **9**, 701 (1989).
[16] G. Servalli and L. Colombo, Europhys. Lett. **22**, 107 (1993).
[17] G. Panzarini and L. Colombo, Phys. Rev. Lett. **73**, 1636 (1994).
[18] A.J. Skinner and D.G. Pettifor, J. Phys.: Condens. Matter **3**, 2029 (1991).
[19] M. Peressi, N. Binggeli, and A. Baldereschi, J. Phys. D **31**, 1273 (1998).
[20] Z. Remes, M. Vanecek, A.H. Mahan, and R.S. Crandall, Phys. Rev. B **56**, 12 710 (1997); Z. Remes, M. Vanecek, P. Torres, U. Kroll, A.H. Mahan, and R.S. Crandall, J. Non-Cryst. Solids **227-330**, 876 (1998); C. Manfredotti and F. Fizzotti, M. Boero, P. Pastorino, P. Polesello, and E. Vittone, Phys. Rev. B **50**, 18 046 (1994).
[21] E. Spanakis, E. Stratakis, and P. Tzanetakis, J. Appl. Phys. **89**, 4294 (2001); P. Danesh, B. Pantchev, D. Grambole, and B. Schmidt, *ibid.* **90**, 3065 (2001).
[22] R. Bellisent, A. Menelle, W.S. Howells, A.C. Wright, T.M. Brunier, R.N. Sinclair, and F. Jansen, Physica B **156&157**, 217 (1989); A. Filipponi, F. Evangelisti, M. Benfatto, S. Mobilio, and C.R. Natoli, Phys. Rev. B **40**, 9636 (1989).
[23] L. Brambilla, L. Colombo, V. Rosato, and F. Cleri, Appl. Phys. Lett. **77**, 2337 (2000).
[24] S. Sriraman, S. Agarwal, E.S. Aydil, and D. Maroudas, Nature (London) **418**, 62 (2002).
[25] M. Fornari, M. Peressi, S. de Gironcoli, and A. Baldereschi, Europhys. Lett. **47**, 481 (1999).
[26] M. Peressi, M. Fornari, S. de Gironcoli, L. De Santis, and A. Baldereschi, Philos. Mag. B **80**, 515 (2000).
[27] M. Fornari, N. Marzari, M. Peressi, and A. Baldereschi, Comput. Mater. Sci. **20**, 337 (2001).
[28] S. Baroni, A. Dal Corso, S. de Gironcoli, and P. Giannozzi, http://www.pwscf.org
[29] X. Gonze, R. Stumpf, and M. Scheffler, Phys. Rev. B **44**, 8503 (1991).
[30] H.J. Monkhorst and J.P. Pack, Phys. Rev. B **13**, 5188 (1976).